

Self-Powered Iontophoretic Transdermal Drug Delivery System Driven and Regulated by Biomechanical Motions

Changsheng Wu, Peng Jiang, Wei Li, Hengyu Guo, Jie Wang, Jie Chen, Mark R. Prausnitz, and Zhong Lin Wang*

Transdermal drug delivery (TDD) systems with feedback control have attracted extensive research and clinical interest owing to their unique advantages of convenience, self-administration, and safety. Here, a self-powered wearable iontophoretic TDD system that can be driven and regulated by the energy harvested from biomechanical motions is proposed for closed-loop motion detection and therapy. A wearable triboelectric nanogenerator (TENG) is used as the motion sensor and energy harvester that can convert biomechanical motions into electricity for iontophoresis without stored-energy power sources, while a hydrogel-based soft patch with side-by-side electrodes is designed to enable noninvasive iontophoretic TDD. Proof-of-concept experiments on pig skin with dyes as model drugs successfully demonstrate the feasibility of the proposed system. This work not only extends the application of TENG in the biomedical field, but may also provide a cost-effective solution for noninvasive, electrically assisted TDD with closed-loop sensing and treatment.

It also avoids the risk of disease transmission by needle reuse and the first-pass hepatic metabolism of drugs. It enables continuous administration of drugs, making it attractive for long-term treatment that reduces the risk of peaks and valleys in drug concentration in the systemic circulation.^[4] The availability of drugs that can be delivered via TDD systems has been extended by various methods of enhancing skin permeability, including the use of chemical molecules, biomolecules and physical tools.^[2] Recent research efforts on TDD has focused on the development of wearable systems with closed-loop sensing and drug delivery.^[4] Advances in wearable biosensors enable sustained, noninvasive, real-time monitoring of human activities and biomarkers

1. Introduction

Transdermal drug delivery (TDD), which refers to the transport of pharmacological agents through the skin typically for systemic administration, has become a common medical practice with over twenty commercially available transdermal drugs approved by the Food and Drug Administration (FDA).^[1–3] Compared to alternatives like oral delivery and hypodermic injection, TDD has many advantages such as being noninvasive, painless, convenient, inexpensive and self-administered.

that can avoid pain and irritation. The biosensing signals collected (e.g., glucose concentration and strain induced by human motions) can be used as feedback control of TDD to achieve on-demand therapeutic delivery.^[5,6] Therefore, the integration of wearable biosensors and TDD provides solutions for precision medicine by achieving closed-loop disease monitoring and therapy, and thus is being actively pursued.

Among the various tools for TDD, iontophoresis has proven to be an effective physical permeation enhancement approach to deliver hydrophilic and/or charged molecules across the skin.^[7–9] An electric current (typically $<0.5 \text{ mA cm}^{-2}$) is applied to the skin to drive the flow of charged molecules by electrophoresis, while the resulting electroosmotic flow of biofluids transports neutral or weakly charged molecules.^[2] Although iontophoretic TDD systems have been commercialized for systemic and local dermal analgesia, local sweat induction and other applications, the use of such electrically controlled patches is hindered by the need of stored-energy power sources that are bulky and costly, as well as requiring complicated electrical components for feedback control.^[10,11] Previously Ogawa et al. reported a completely organic iontophoresis patch with a built-in biofuel cell as a lightweight and safe power source, but it did not offer feedback control since the current could not be adjusted once the patch was mounted on the skin.^[12]

Meanwhile, triboelectric nanogenerator (TENG), which can convert mechanical energy into electricity through the coupled effects of triboelectrification and electrostatic induction, has emerged as a promising power source for the era of internet of things owing to its merits of low cost, broad material availability,

Dr. C. Wu, Dr. P. Jiang, Dr. H. Guo, J. Chen, Prof. Z. L. Wang
School of Materials Science and Engineering
Georgia Institute of Technology
Atlanta, GA 30332, USA
E-mail: zhong.wang@mse.gatech.edu

Dr. P. Jiang
Wuhan University School of Pharmaceutical Sciences
Wuhan 430071, P. R. China

Dr. W. Li, Prof. M. R. Prausnitz
School of Chemical and Biomolecular Engineering
Georgia Institute of Technology
Atlanta, GA 30332, USA

Dr. J. Wang, Prof. Z. L. Wang
Beijing Institute of Nanoenergy and Nanosystems
Chinese Academy of Sciences
Beijing 100083, P. R. China

 The ORCID identification number(s) for the author(s) of this article can be found under <https://doi.org/10.1002/adfm.201907378>.

DOI: 10.1002/adfm.201907378

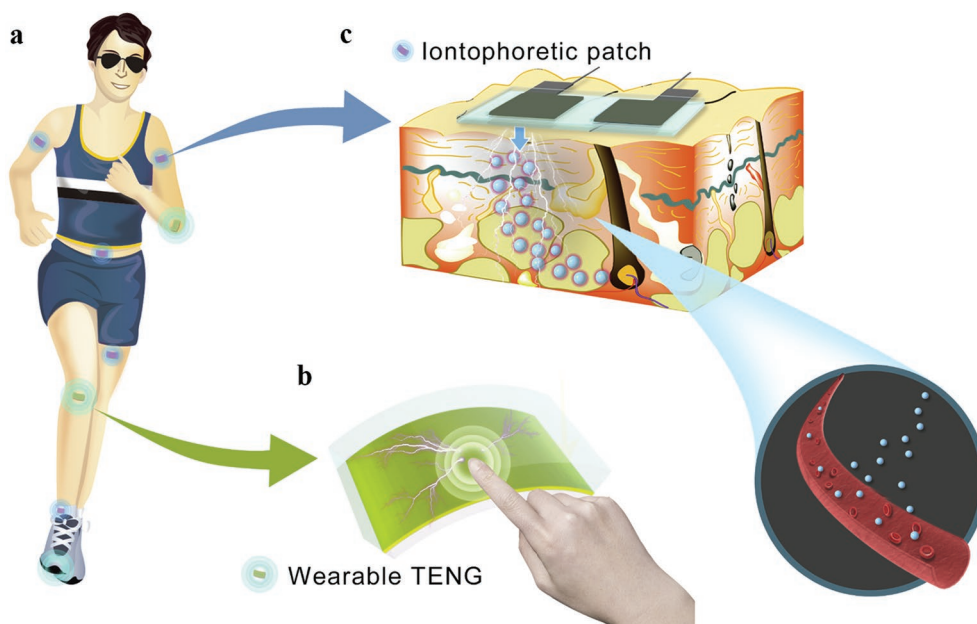


Figure 1. Schematic of self-powered iontophoretic TDD system. a) Person in motion wearing the TDD devices. b) Illustration of wearable TENG device for motion detection and biomechanical energy harvesting. c) Illustration of drug patch that delivers drug to skin via iontophoresis.

light weight, and high efficiency at low operation frequency.^[13] It has found many potential applications as a micropower source for self-powered wearable or implantable systems.^[14–18] Recently, TENG was also proposed as a voltage source for electroporation-mediated drug delivery using a system that requires invasive penetration of a metallic electrode under the skin to deliver molecules into cells in the skin.^[19]

To address the issues of power source and feedback control in iontophoretic TDD and the issue of invasiveness in TENG-driven electroporation-mediated drug delivery, a self-powered wearable iontophoretic TDD system based on biomechanical motion sensing and energy harvesting is proposed in this work for closed-loop motion detection and therapy. Such a system has the advantages of conventional iontophoretic TDD, in addition to requiring no stored-energy power source such as a battery and enabling responsive drug delivery stimulated by biomechanical motion.

2. Results and Discussion

To realize a wearable iontophoretic TDD system that offers on-demand therapeutic delivery without stored-energy power sources, our proposed system consists of a wearable TENG as the integrated power source and a hydrogel-based soft patch as the drug carrier (Figure 1). The TENG can be designed in various form factors and mounted onto different parts of the body to scavenge electric energy from biomechanical motions. The rationally designed drug patch is made of soft materials and can be conformally attached onto the targeted spots on human skin (Figure 1c).

The drug patch is electrically connected to the TENG, and thus the TENG output, which is stimulated by body motions, can be used to accelerate the transdermal drug delivery rate via iontophoresis without stored-energy power sources. Since the

body motions for TENG operation can be either involuntary (e.g., breathing and tremor) or intentional (e.g., arm bending and walking), this self-powered TDD system offers the options of sustained drug release and intentional drug release with feedback control. For example, the involuntary motions of a patient with tremor can trigger the TENG operation and facilitate on-demand drug release to treat the tremor, while patients with ankle injury can receive extra dosing of analgesic automatically during walking when the TENG is mounted on the foot.

The feasibility of using TENG to power iontophoretic TDD was first investigated via the study of the electrophoretic flow driven by TENG (Figure 2). A customized diffusion cell consisting of four unit cells separated by three cellulose membranes, was fabricated as the experimental apparatus (Figure 2a). The two inner cells, i.e., the donor cell and the acceptor cell, were separated by a cellulose membrane with a pore size of 3 μm , while the two outer cells were separated from the inner cells by cellulose membranes with a pore size of 0.45 μm and worked as buffer layers to minimize the electrolysis of test molecules by the electrodes.

At the beginning of tests, all four cells were filled with the same amount of liquid (1 mL), with only the donor cell having the PBS solution containing test molecules and the other three having just PBS solution. A contact-separation-mode TENG^[20–22] (Figure S1, Supporting Information), where polytetrafluoroethylene (PTFE) was used as one triboelectric material and aluminum (Al) as the other triboelectric material and electrodes, was used in the tests and operated by an electrodynamic shaker. The TENG was connected to the two carbon-cloth electrodes of the customized diffusion cell through a rectifier, which converted the alternating current output of TENG into direct-current electricity.

Rhodamine 6G (R6G), a cationic fluorescent organic dye with maximum absorption at 530 nm and emission at 556 nm (Figure 2b), and methylene blue (MB), a cationic medication

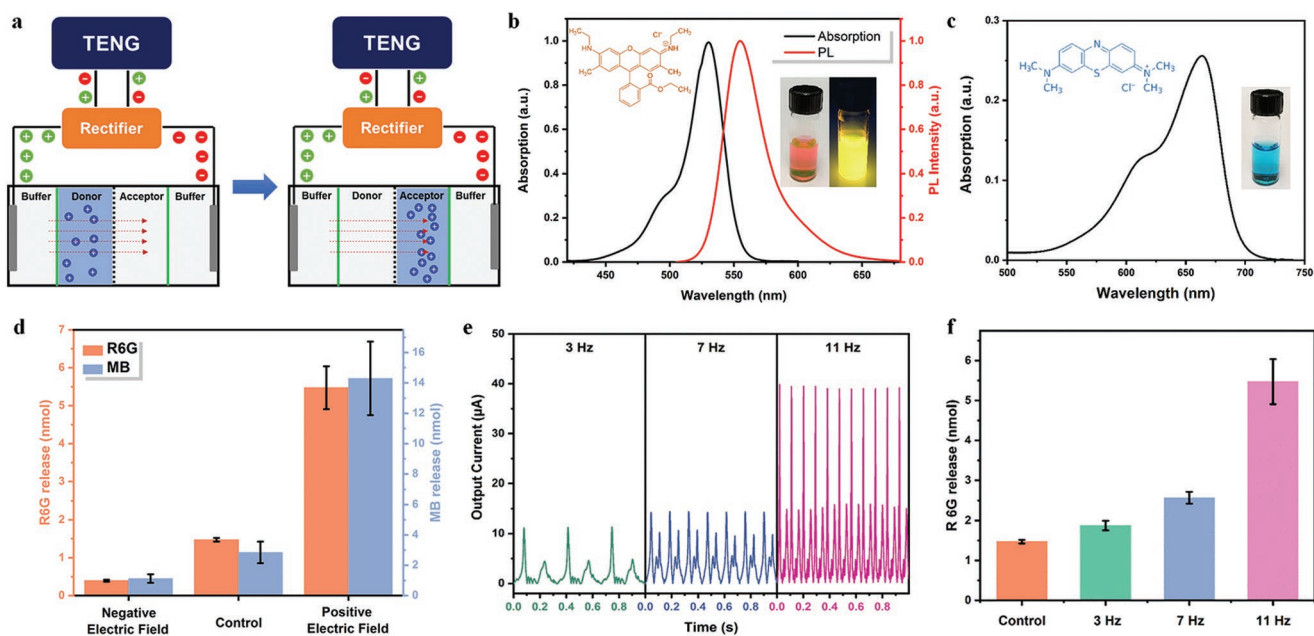


Figure 2. Study of electrophoretic flow driven by TENG. a) Schematic of experimental setup using a diffusion cell. b) Representative absorption and fluorescence spectra, structural formula (inset, left), bright-field and fluorescence photographs (inset, right) of R6G. c) Representative absorption spectrum, structural formula (inset, left), bright-field photograph (inset, right) of MB. d) Effects of electric field direction on transport of R6G and MB. e) Representative output currents of TENG under different operation frequencies. f) Effects of TENG operation frequency on diffusion of R6G. Bar graphs show mean \pm SD ($n = 5$ independent replicate experiments).

and dye with maximum absorption at 665 nm (Figure 2c), were used as the test materials. In clinical practice, MB is used to treat methemoglobinemia, urinary tract infections and cyanide poisoning, and is under study for treatment of Alzheimer's disease.^[23]

The effects of electric field direction from TENG on the dye transport rate was first studied, with experimental results shown in Figure 2d and Figure S2 (Supporting Information). The concentration of R6G and MB in the acceptor cell was calculated from calibration curves prepared with standard solutions (Figure S3, Supporting Information). Under a positive electric field (from the donor cell to the acceptor cell), the transported amount of dye molecules in the acceptor cell increased significantly after 30 min of TENG operation at a frequency of 11 Hz, while the amount decreased when the electric field was reversed. This relationship between transport rate and electric field direction applied to both R6G and MB, and fit well with our expectation. A positive current accelerated the flow of positively charged dye molecules in the PBS solution from the donor cell to the acceptor cell. Meanwhile, an opposite current hindered the transport of dye molecules driven by concentration difference, resulting in a smaller transport rate.

The effects of TENG operation frequency on the transport rate were studied as well. Figure 2e shows the current flowing through the diffusion cell when the TENG operated at different frequencies. Higher operation frequency brought higher number and larger amplitude of current peaks, which resulted in a larger driving force for the electrophoretic flow and thus a faster transport rate of the targeted molecules, as evidenced by the amount of transported R6G in Figure 2f after 30 min of TENG operation at different frequencies.

To realize the proposed self-powered iontophoretic TDD in a noninvasive manner, a hydrogel-based drug patch was designed and fabricated (Figure 3a; Figure S4, Supporting Information). The drug patch consists of two side-by-side hydrogel cells and two embedded carbon-cloth electrodes in a polydimethylsiloxane (PDMS) frame. Therapeutic agents are preloaded into one of the hydrogel cells during fabrication. Owing to its soft mechanical property and biocompatibility, hydrogels have been widely adopted as a delivery medium for iontophoresis. Along with soft PDMS as the main substrate, the whole device could conformably attach to the skin and enable drug release in a convenient and comfortable manner.

Poloxamer 407-based hydrogel, which is thermosensitive and has been used in FDA-approved products,^[24] was used in this study. Because of hydrophobic interactions between the copolymer chains, poloxamer 407 aqueous solutions (20–30 wt%) exhibited reversible thermogelation properties, which has been characterized by the concentration-dependent sol–gel transition temperature ($T_{\text{sol-gel}}$).^[25] The solutions switch between fluid and semisolid states when the temperature changes near the $T_{\text{sol-gel}}$, as illustrated in Figure 3b.^[24,26] This reversible sol-gel property gives poloxamer 407 hydrogel advantages in TDD applications, such as easy drug loading, good contact with skin, and easy removal from the skin. Furthermore, its good electrical conductivity makes it suitable for iontophoresis. Figure 3c presents images of poloxamer 407 solutions loaded with R6G ($60 \mu\text{mol L}^{-1}$) and MB ($60 \mu\text{mol L}^{-1}$), which show their transition between fluid and semisolid states as the temperature changes.

The poloxamer 407 solutions with and without dye loading were dispensed into the two cells of the PDMS frame on top of the carbon-cloth electrodes at a low temperature (4°C), followed by thermogelation at 37°C . The optical and fluorescent

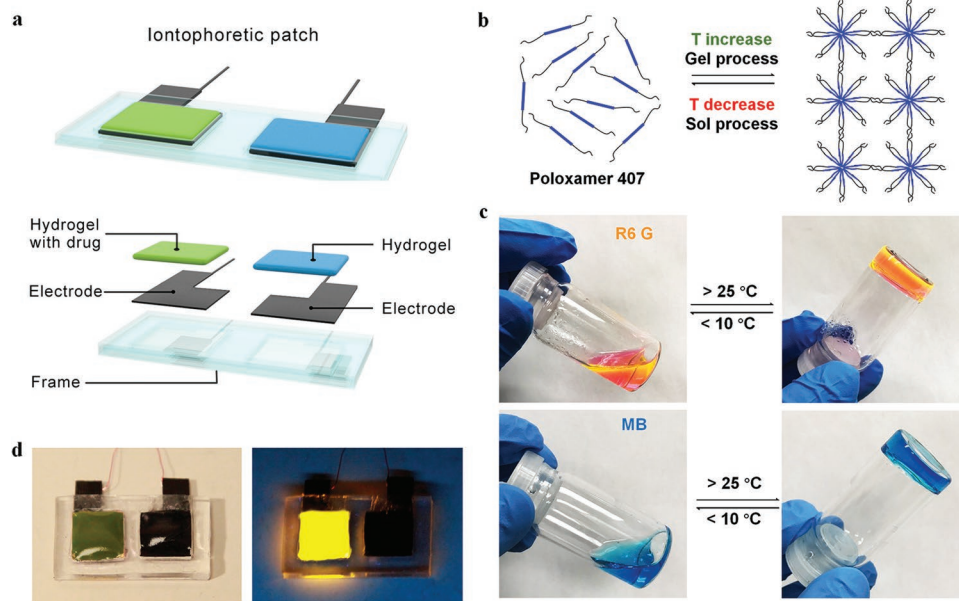


Figure 3. Hydrogel-based soft patch for TDD. a) Schematic of the device structure. b) Schematic of gelation and solution process of hydrogel.^[24,26] c) Photographs of hydrogel loaded with different dyes. d) Photographs of fabricated device with R6G as simulated drug under normal ambient light (left) and ultraviolet light showing R6G fluorescence (right).

images of the fabricated iontophoretic drug patch with R6G as the simulated drug are presented in Figure 3d. Both the dark green (from the combination of black from the electrode and orange from R6G) color region in the optical image and the bright yellow region in the fluorescent image under an ultraviolet (UV, 365 nm) lamp indicate the uniform existence of R6G in the left hydrogel cell.

Wearable TENG, which can take various forms including textile,^[27–29] insole,^[30–32] wristband,^[14] e-skin,^[33] etc. (Figure 4a), offers a promising solution for self-powered wearable systems by converting biomechanical energy into electrical energy. In this work, a wearable insole TENG was fabricated for the proof-of-concept demonstration. As illustrated in Figure 4b, the insole TENG used PTFE as one triboelectric material, Al as the other triboelectric material and electrodes, polyethylene terephthalate (PET) as the substrate, and Kapton as the spacer. Its working mechanism is illustrated in Figure S5 (Supporting Information) using a representative single unit. When the foot steps onto it, the PTFE and Al come into contact and opposite charges are induced on their surfaces. These induced charges drive current to flow between the Al electrodes through an external circuit when the gap distance between PTFE and Al changes. Multiple units can be integrated together as in Figure 4b to enhance the electrical outputs, and a device with three units was used for our experiments.

Combined with the wearable hydrogel-based drug patch, such a TENG device can be deployed onto the human body to make a self-powered electrically assisted TDD system. In the case of cationic drugs (like the model drugs R6G/MB), the electrode on the drug-containing hydrogel is connected to the positive terminal of a rectifier that converts the AC output of TENG into DC current, while the other electrode is connected to the negative terminal to form a complete circuit. If oppositely charged ionic drugs are used, cationic and anionic drugs will be load

into the cell connected to the positive and negative terminal, respectively. As a result, the TENG output, which is stimulated by body motions (e.g., walking), can be used to accelerate the transdermal drug release rate via iontophoresis without stored-energy power sources. Figure 4c demonstrates the concept of a pain-relief TDD system for ankle injury, with the drug patch on the ankle and an insole TENG under the shoe. The drug can be administered on-demand when the patient walks on his or her foot and generates electricity at the same time. The typical electrical outputs of the insole TENG consisting of three units connected in parallel under open-circuit and short-circuit conditions are plotted in Figure 4d. Its open-circuit voltage reached ≈ 1200 V, short-circuit charge transfer was ≈ 370 nC per cycle, and maximum short-circuit current was nearly $20 \mu\text{A}$ at an operation frequency of 2 Hz.

To better evaluate the performance of the TENG-driven iontophoretic TDD system, it was applied to pig skin, which is commonly used as a surrogate for human skin, using R6G as the model drug loaded in one hydrogel cell (Figure 5a). Since the model drug R6G is cationic, the drug patch was connected to the TENG via a rectifier, with the electrode on the dye-loading cell wired to the positive terminal and the other electrode to the negative terminal. The insole TENG was operated using a linear motor at a frequency of 2 Hz to mimic human walking behavior, and the drug patch was placed in a 37°C oven during the drug delivery experiment to simulate body temperature. The electrical outputs of the TENG under such a load condition (drug patch and pig skin) were measured, with its $V-Q$ plot shown in Figure 5b. Approximately 320 nC of charge was transferred per operation cycle and an AC peak-to-peak output voltage with an amplitude of 8 V was achieved. After the rectifier, a pulsed DC current with a maximum of $\approx 12 \mu\text{A}$ was delivered to the designed hydrogel device at a maximum voltage of 4 V (Figure 5c). During operation, the electrical outputs from

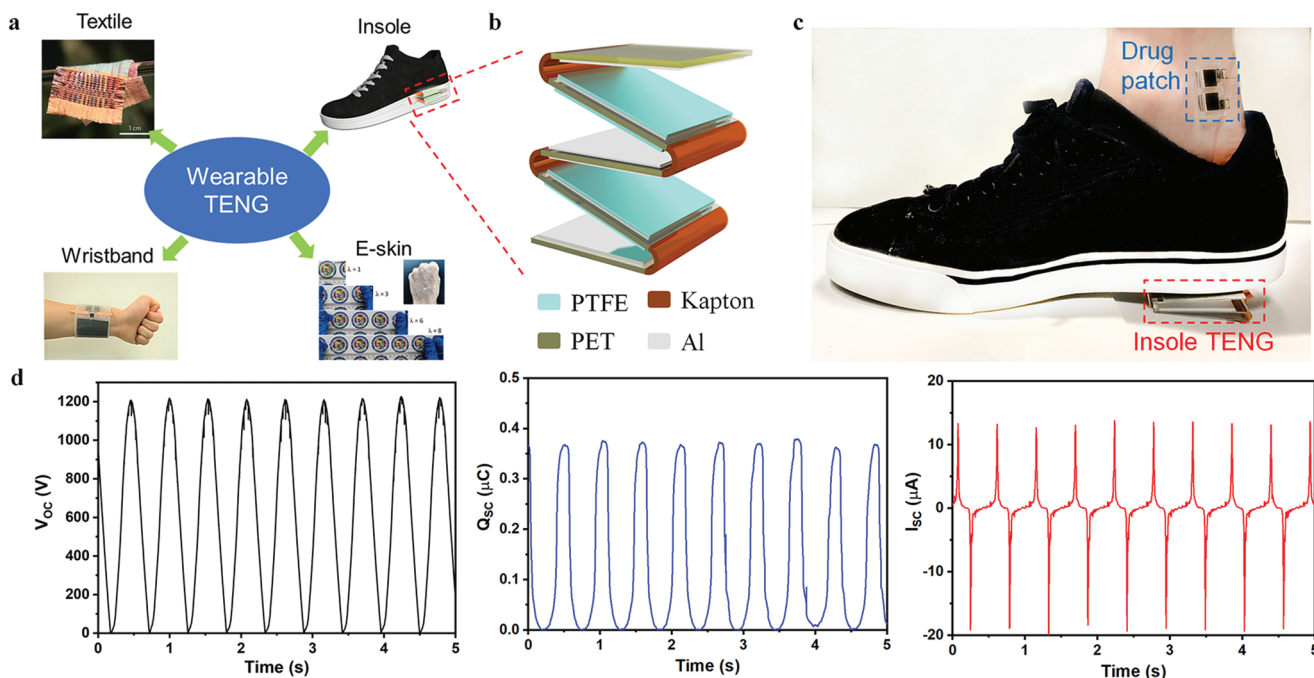


Figure 4. Wearable TENG for harvesting biomechanical energy to drive electrically assisted TDD. a) Examples of wearable TENG. Reproduced with permission.^[27] Copyright 2016, Springer Nature. Reproduced with permission.^[14] Copyright 2018, Elsevier. Reproduced under the terms of the CC-BY-NC 4.0 License.^[33] Copyright 2017, The American Association for the Advancement of Science. b) Schematic of the insole TENG used in this study. c) Photograph demonstrating the idea of a wearable TDD system on a human ankle consisting of the insole TENG and designed drug patch. d) Representative electrical outputs of the insole TENG under open-circuit and short-circuit conditions. V_{OC} is open-circuit voltage, Q_{SC} is short-circuit charge transfer, and I_{SC} is short-circuit current.

TENG would drive the ions inside the hydrogel drug patch to flow from one cell to the other. Since the two cells were insulated from each other by the PDMS frame, the routes of the least electrical resistance would be through the skin. As a result, the model drugs (R6G/MB) would be transported into the skin via this electrical flow and TDD via iontophoresis was achieved.

The drug patch was left on the skin with the TENG in continuous operation for 6 h before examination (Figure 5d), and a control experiment was performed under identical conditions except that the TENG was not connected (Figure 5h). The fluorescent images under the 365 nm UV lamp (Figure 5e,i) showed that the fluorescence of R6G delivered into the skin from the TENG-driven device was much stronger than the control, and the emission of fluorescence was seen primarily from the part of the skin that was under the cathode, which is consistent with electrophoresis of positively charged R6G.

Cross-sectional histological images were then taken to further compare the results. The distinct contrast between the fluorescent cross-sectional images (Figure 5g,k) presented additional evidence that more R6G was released into the skin from the TENG-driven device and the R6G was delivered more deeply into the skin with TENG. Another set of comparison experiments was conducted using MB as the simulated drug, with the results shown in Figure S6 (Supporting Information). The surface area of the skin treated by the TENG-driven TDD system was darker than that of the control group, indicating that more MB was delivered into the skin in the TENG-driven experiment. Altogether, the results here demonstrate

the feasibility of the proposed self-powered iontophoretic TDD system driven by biomechanical motion, through the integration of a wearable TENG and an electrically assisted drug patch.

3. Conclusion

In this study, a self-powered, noninvasive TDD system consisting of a wearable TENG and an iontophoretic patch was proposed and developed. The emerging TENG technology offers a facile and cost-effective solution for wearable energy harvesters that can detect body motion and convert associated biomechanical energy into electricity simultaneously, while the hydrogel-based drug patch enables TDD from a thin, conformal skin patch made of biocompatible materials. The feasibility of the proposed system was demonstrated on pig skin using dyes as simulated drugs, with both bright-field and fluorescence images indicating that the TENG outputs drove transport of the model drugs into the skin.

It is worth noting that the insole TENG used in this work was not optimized and recent advances in shape-adaptive and fiber-based TENG are expected to further enhance the energy conversion efficiency and thus the driving force for iontophoretic TDD. Due to the variability of skin resistance among different people, skin sites, and skin status, however, it would require more sophisticated and power-consuming control circuitry when the dosing rate and amount need to be exact. Depending on the application scenario where the triggering motion of TENG can be either involuntary or intentional, both

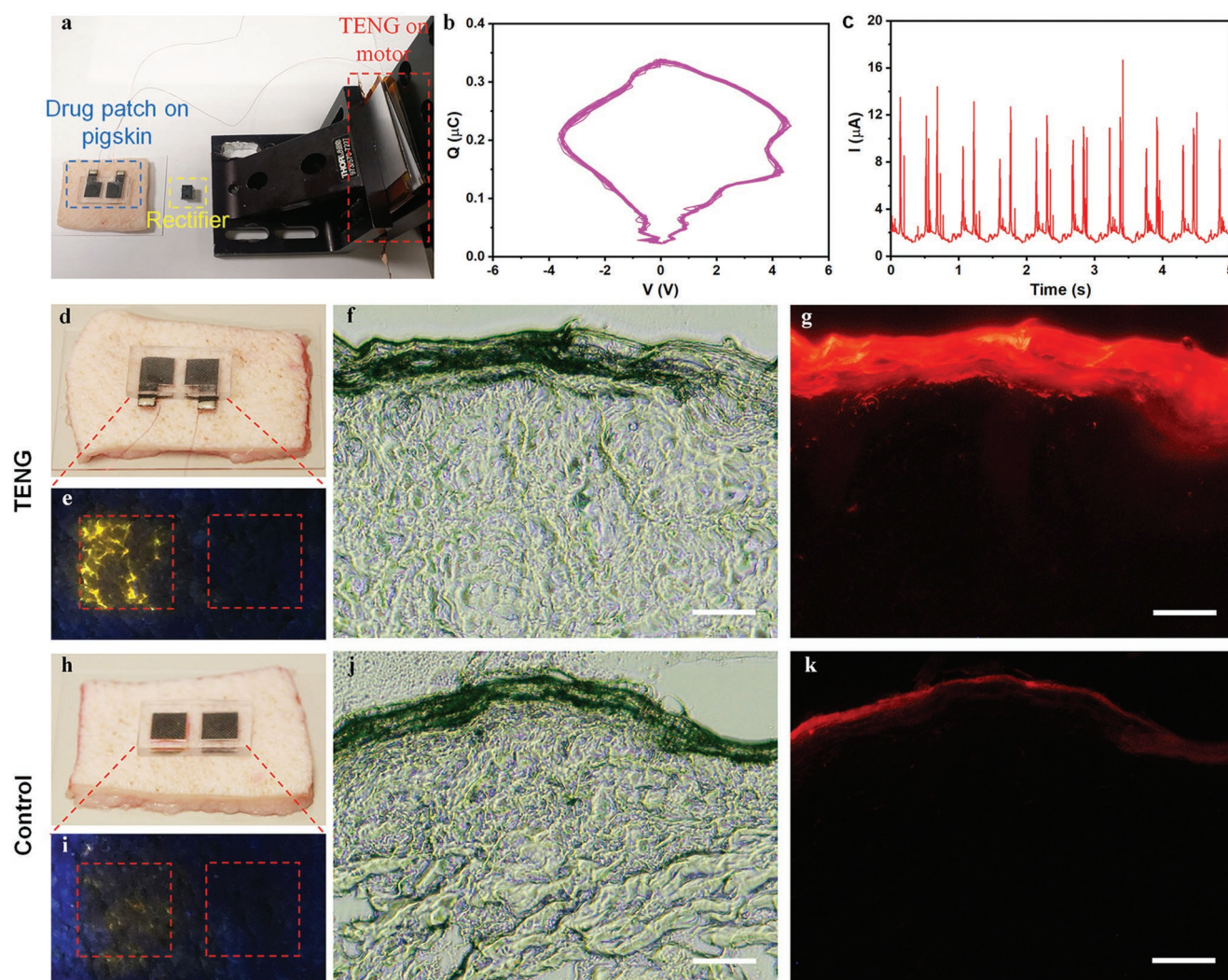


Figure 5. Proof-of-concept demonstration of self-powered TDD system on pig skin. a) Photograph of the experimental setup with foot motion simulated by a linear motor; b) representative $V-Q$ (voltage–charge) plot of the corresponding TENG output; c) representative rectified current (I) that passed through the designed hydrogel device and skin. Photograph of the R6G-containing hydrogel drug patch on skin d) with and h) without TENG connection. Representative en face fluorescence images e,i), bright-field cross-sectional histological images f,j), and fluorescent cross-sectional histological images g,k) of skin after R6G delivery from a patch for 6 h with e–g) and without i–k) TENG connection. Scale bar, 50 μm .

sustained drug release and triggered release with feedback control can be achieved.

This advanced TDD system is expected to be cost-effective without complicated components, and the modular design enables reuse of the TENG power component with different drug patches. Therefore, this work provides a promising solution for noninvasive, electrically assisted TDD with closed-loop sensing and treatment, and promotes TENG-based self-powered systems toward advanced biomedical treatment.

4. Experimental Section

Fabrication of TENG: Two different TENGs were fabricated in this work. The first TENG was a spring-based contact-separation TENG for the study of electrophoretic flow in Figure 2, which was fabricated using methods similar to those in previous reports.^[34,35] Two acrylic

plates (15 cm wide \times 15 cm long \times 0.32 cm thick; McMaster-Carr, Elmhurst, IL) were used as the substrates. A PTFE film (10 cm wide \times 10 cm long \times 50 μm thick; American Durafilm, Holliston, MA) and an Al film (10 cm wide \times 10 cm long \times 100 μm thick; McMaster-Carr, Elmhurst, IL) were pasted on one acrylic plate using double-sided Kapton polyimide tape (Ted Pella, Redding, CA), and an Al film (10 cm wide \times 10 cm long \times 100 μm thick) on the other plate. Four springs (9657K301; McMaster-Carr, Elmhurst, IL) were fixed at the four corners of the acrylic plates using epoxy glue (Loctite, Westlake, OH) to work as the spacer. The TENG was operated using an electrodynamic shaker (Labworks Inc., Costa Mesa, CA) at different frequencies. The second TENG was a wearable insole TENG for TDD experiments. It used PTFE as one triboelectric material, Al as the other triboelectric material and electrodes, PET as the substrate, and Kapton as the spacer. Three units were integrated together like the schematic in Figure 4b (where four units are illustrated) and electrically connected in parallel. The TENG was operated using a linear motor (H01-48 \times 370/90, LinMot, Lake Geneva, WI).

Electrical Measurements: Electrical measurements were conducted using the Keithley 6514 Electrometer (Keithley Instruments, Cleveland,

OH). The electrical circuit model for measuring the $V-Q$ plot and rectified current in Figure 4f,g is drawn in Figure S7 (Supporting Information).

Preparation of Hydrogel Solutions: Briefly, poloxamer 407 (Sigma, St. Louis, MO) was added to deionized water in an ice bath with the final poloxamer 407 concentration at 25 wt% under continuous magnetic stirring. The solution was then refrigerated until poloxamer 407 was completely dissolved and a clear solution was obtained. For dye-loading solutions, a R6G (Alfa Aesar, Ward Hill, MA) or MB (Sigma-Aldrich) aqueous solution was prepared in deionized water and added to the poloxamer 407 solution to achieve a final R6G (or MB) concentration of $60 \mu\text{mol L}^{-1}$.

Fabrication of Hydrogel-Based Iontophoretic Drug Patch: The detailed fabrication process of the hydrogel-based iontophoretic drug patch is illustrated in Figure S4 (Supporting Information). An acrylic mold was first fabricated via laser cutting and glue assembly. Sylgard 184 (Dow Corning, Midland, MI), with a weight ratio of 10:1 for Part A:Part B, was cast into the acrylic mold and cured at 50°C for 24 h to produce the PDMS frame. The PDMS frame had two side-by-side cells with dimensions of 10 mm wide \times 10 mm long \times 1.5 mm deep. The dye-loaded poloxamer 407 solution was poured into one cell of the mold and plain poloxamer 407 solution into the other cell. Finally, the patch was placed in a 37°C oven for the thermal gelation.

Evaluation of the Performance of the TENG-Driven Drug Patch on Pig Skin: The drug patch fabricated above was placed on pig skin with the TENG in continuous operation for 6 h, and a control experiment was performed under identical conditions except that the TENG was not connected. The pig skin was obtained from slaughterhouse, which was exempt from approval by the Institutional Animal Care and Use Committee at Georgia Tech. The skin was then embedded in optimal-cutting-temperature compound (OCT, Tissue-Tek, Torrance, CA), frozen at -80°C for 15 min and sliced into $10 \mu\text{m}$ sections using a cryostat. Slides were then imaged using a fluorescence microscope (Olympus IX70, Tokyo, Japan).

Supporting Information

Supporting Information is available from the Wiley Online Library or from the author.

Acknowledgements

C.W. and P.J. contributed equally to this work. This research was supported by the Hightower Chair foundation and China National Mega-Projects for Infectious Diseases (No. 2018ZX10301405). P. Jiang acknowledges the China Scholarship Council and Wuhan University for supporting research at Georgia Institute of Technology.

Conflict of Interest

The authors declare no conflict of interest.

Keywords

energy harvesting, iontophoresis, self-power, transdermal drug delivery, triboelectric nanogenerator

Received: September 6, 2019

Revised: October 2, 2019

Published online:

[1] M. R. Prausnitz, R. Langer, *Nat. Biotechnol.* **2008**, *26*, 1261.

[2] R. Yang, T. Wei, H. Goldberg, W. Wang, K. Cullion, D. S. Kohane, *Adv. Mater.* **2017**, *29*, 1606596.

- [3] O. S. Fenton, K. N. Olafson, P. S. Pillai, M. J. Mitchell, R. Langer, *Adv. Mater.* **2018**, *30*, 1705328.
- [4] M. Amjadi, S. Sheykhsari, B. J. Nelson, M. Sitti, *Adv. Mater.* **2018**, *30*, 1704530.
- [5] H. Lee, T. K. Choi, Y. B. Lee, H. R. Cho, R. Ghaffari, L. Wang, H. J. Choi, T. D. Chung, N. Lu, T. Hyeon, S. H. Choi, D.-H. Kim, *Nat. Nanotechnol.* **2016**, *11*, 566.
- [6] J. Di, S. Yao, Y. Ye, Z. Cui, J. Yu, T. K. Ghosh, Y. Zhu, Z. Gu, *ACS Nano* **2015**, *9*, 9407.
- [7] Y. N. Kalia, A. Naik, J. Garrison, R. H. Guy, *Adv. Drug Delivery Rev.* **2004**, *56*, 619.
- [8] Y. T. Yi, J. Y. Sun, Y. W. Lu, Y. C. Liao, *Biomicrofluidics* **2015**, *9*, 022401.
- [9] K. Ita, *Int. J. Pharm.* **2015**, *496*, 240.
- [10] K. Ita, *J. Drug Targeting* **2016**, *24*, 386.
- [11] P. C. Pandey, S. Shukla, S. A. Skoog, R. D. Boehm, R. J. Narayan, *Sensors* **2019**, *19*, 1028.
- [12] Y. Ogawa, K. Kato, T. Miyake, K. Nagamine, T. Ofuji, S. Yoshino, M. Nishizawa, *Adv. Healthcare Mater.* **2015**, *4*, 506.
- [13] C. Wu, A. C. Wang, W. Ding, H. Guo, Z. L. Wang, *Adv. Energy Mater.* **2019**, *9*, 1802906.
- [14] Q. Jiang, C. Wu, Z. Wang, A. C. Wang, J.-H. He, Z. L. Wang, H. N. Alshareef, *Nano Energy* **2018**, *45*, 266.
- [15] X. He, Y. Zi, H. Guo, H. Zheng, Y. Xi, C. Wu, J. Wang, W. Zhang, C. Lu, Z. L. Wang, *Adv. Funct. Mater.* **2017**, *27*, 1604378.
- [16] Y.-C. Lai, J. Deng, S. Niu, W. Peng, C. Wu, R. Liu, Z. Wen, Z. L. Wang, *Adv. Mater.* **2016**, *28*, 10024.
- [17] Q. Zheng, Y. Zou, Y. Zhang, Z. Liu, B. Shi, X. Wang, Y. Jin, H. Ouyang, Z. Li, Z. L. Wang, *Sci. Adv.* **2016**, *2*, e1501478.
- [18] P. Song, S. Kuang, N. Panwar, G. Yang, D. J. H. Tng, S. C. Tjin, W. J. Ng, M. B. A. Majid, G. Zhu, K.-T. Yong, Z. L. Wang, *Adv. Mater.* **2017**, *29*, 1605668.
- [19] Z. Liu, J. Nie, B. Miao, J. Li, Y. Cui, S. Wang, X. Zhang, G. Zhao, Y. Deng, Y. Wu, Z. Li, L. Li, Z. L. Wang, *Adv. Mater.* **2019**, *31*, 1807795.
- [20] J. Wang, C. Wu, Y. Dai, Z. Zhao, A. Wang, T. Zhang, Z. L. Wang, *Nat. Commun.* **2017**, *8*, 88.
- [21] Y. Zi, C. Wu, W. Ding, Z. L. Wang, *Adv. Funct. Mater.* **2017**, *27*, 1700049.
- [22] C. Wu, W. Ding, R. Liu, J. Wang, A. C. Wang, J. Wang, S. Li, Y. Zi, Z. L. Wang, *Mater. Today* **2018**, *21*, 216.
- [23] M. Oz, D. E. Lorke, G. A. Petroianu, *Biochem. Pharmacol.* **2009**, *78*, 927.
- [24] G. Dumortier, J. L. Grossiord, F. Agnely, J. C. Chaumeil, *Pharm. Res.* **2006**, *23*, 2709.
- [25] A. Fakhari, M. Corcoran, A. Schwarz, *Heliyon* **2017**, *3*, e00390.
- [26] W. Wang, E. Wat, P. C. L. Hui, B. Chan, F. S. F. Ng, C.-W. Kan, X. Wang, H. Hu, E. C. W. Wong, C. B. S. Lau, P.-C. Leung, *Sci. Rep.* **2016**, *6*, 24112.
- [27] J. Chen, Y. Huang, N. Zhang, H. Zou, R. Liu, C. Tao, X. Fan, Z. L. Wang, *Nat. Energy* **2016**, *1*, 16138.
- [28] X. Pu, L. Li, H. Song, C. Du, Z. Zhao, C. Jiang, G. Cao, W. Hu, Z. L. Wang, *Adv. Mater.* **2015**, *27*, 2472.
- [29] X. Pu, L. Li, M. Liu, C. Jiang, C. Du, Z. Zhao, W. Hu, Z. L. Wang, *Adv. Mater.* **2016**, *28*, 98.
- [30] J. Wang, S. Li, F. Yi, Y. Zi, J. Lin, X. Wang, Y. Xu, Z. L. Wang, *Nat. Commun.* **2016**, *7*, 12744.
- [31] S. Niu, X. Wang, F. Yi, Y. S. Zhou, Z. L. Wang, *Nat. Commun.* **2015**, *6*, 8975.
- [32] G. Zhu, P. Bai, J. Chen, Z. Lin Wang, *Nano Energy* **2013**, *2*, 688.
- [33] X. Pu, M. Liu, X. Chen, J. Sun, C. Du, Y. Zhang, J. Zhai, W. Hu, Z. L. Wang, *Sci. Adv.* **2017**, *3*, e1700015.
- [34] J. Chen, G. Zhu, W. Yang, Q. Jing, P. Bai, Y. Yang, T.-C. Hou, Z. L. Wang, *Adv. Mater.* **2013**, *25*, 6094.
- [35] G. Zhu, Z.-H. Lin, Q. Jing, P. Bai, C. Pan, Y. Yang, Y. Zhou, Z. L. Wang, *Nano Lett.* **2013**, *13*, 847.